

Field-Induced Discommensuration in Charge Density Waves in *o*-TaS₃

Katsuhiko INAGAKI*, Masakatsu TSUBOTA, Kazuki HIGASHIYAMA, Koichi ICHIMURA,
Satoshi TANDA, Kenichiro YAMAMOTO¹, Noriaki HANASAKI¹, Naoshi IKEDA¹,
Yoshio NOGAMI¹, Takayoshi ITO², and Hidenori TOYOKAWA²

Division of Applied Physics, Graduate School of Engineering, Hokkaido University, Kita 13 Nishi 8, Kita-ku, Sapporo 060-8628

¹*Graduate School of Natural Science and Technology, Okayama University, 3-1-1 Tsushima-naka, Okayama 700-8530*

²*Japan Synchrotron Radiation Research Institute, 1-1-1 Koto, Sayo, Hyogo 679-5198*

(Received March 28, 2008; accepted July 22, 2008; published September 10, 2008)

We report a synchrotron X-ray study of charge density waves (CDWs) in an *o*-TaS₃ crystal. We found that two independent CDWs coexist in the temperature range of 130–50 K. These waves are incommensurate and commensurate CDWs with longitudinal wave vectors $q_c = 0.252c^*$ and $0.250c^*$, respectively. The temperature and electric current dependences of the intensity of the two CDW satellites were measured. We found that the commensurate CDW was converted to the incommensurate CDW at 80 K by inducing current flow. Our observation was interpreted in terms of the dynamics of topological defects. We determined the edge dislocation configuration from the electric current dependence of the intensity of the two CDWs. The result implies for the first time that discommensurations are induced in the commensurate CDW by applying an electric field.

KEYWORDS: charge density wave, *o*-TaS₃, discommensuration

DOI: [10.1143/JPSJ.77.093708](https://doi.org/10.1143/JPSJ.77.093708)

Dislocations on the macroscopic order are an attractive subject, particularly when they become ordered and exhibit a new spatial periodicity. A well-known example is the mixed state of a superconductor under a modest magnetic field, where vortices form the Abrikosov lattice.¹⁾ A dual phenomenon is predicted in charge density waves (CDWs): that is, when an electric field is applied perpendicularly to the CDW chain direction, dislocations can enter the CDW to form a mixed state as a type-II superconductor.²⁾

Since the degree of freedom of the CDW order parameter is larger than that of a conventional superconductor,³⁾ one can expect to observe more variety of dislocations, by analogy of ³He superfluids and liquid crystals. Moreover, in contrast to superconducting vortices, which have no effect on X-rays and therefore cannot be studied using them, the order parameter of a CDW couples with the lattice distortion and modifies diffraction; hence, high-resolution synchrotron studies can now be conducted.⁴⁻⁶⁾

In this article, we report the discovery of a mixed state as a result of our synchrotron X-ray study of CDWs in *o*-TaS₃ performed at SPring-8. We measured the temperature dependence of Bragg and satellite peak profiles precisely down to 7.3 K with and without current flowing through the sample. We found that at 50–130 K, the mixed state exists stably with the coexistence of two kinds of CDWs, attributed to the commensurate and incommensurate wave vectors. From the electric current dependence of the intensity of the two CDWs, we demonstrated the evolution of edge dislocations of CDW, i.e., discommensurations.⁷⁾ The result implies that the dislocations are induced in the commensurate CDW by applying an electric field *along the chain direction*. This is the first such report for a CDW.

We investigated a quasi-one-dimensional conductor *o*-TaS₃ on its CDW properties. It undergoes a Peierls transition at $T_P \sim 218$ K to an incommensurate CDW. In contrast to similar materials, e.g., NbSe₃, the whole Fermi surface of

o-TaS₃ contributes to the transition. In a previous X-ray study,⁸⁾ it was shown that the CDW wave vector q at temperatures around T_P is incommensurate, $q_c \sim (0.255 \pm 0.003)c^*$, and by reducing temperature it becomes nearly commensurate below 100 K, where $q_c \sim (0.250 \pm 0.004)c^*$.

The single crystal of *o*-TaS₃ used in this study was synthesized by the standard chemical vapor transport method. The reaction and crystal growth were undertaken in an evacuated quartz tube using tantalum and sulfur powder. A piece of ribbonlike crystal was then placed on a copper sample holder with an insulating glass layer. The sample dimensions were 5 mm \times 12 μ m \times 27 μ m. A gold film was then deposited on the crystal and electrodes were formed using silver paste. Electric current was fed from a low-level current generator (Keithley 6221), while the voltage drop at the sample was monitored with a high-impedance voltmeter (Keithley 617) to prevent the voltmeter from shunting the sample current.

The X-ray study was performed at BL02B1 of SPring-8. The incident beam passed through a double-crystal monochromator. The wavelength was 0.61984(89) Å, which was calibrated with standard CeO₂ powder prior to the measurement. A synchrotron beam of 0.5 mm diameter was irradiated through a hole of the sample holder. The irradiated area of the sample was 1.3 mm away from the electrodes.⁹⁾ Diffraction was monitored with a position-sensitive two-dimensional detector, Pilatus-100K,¹⁰⁾ located 1303.7 mm away from the rotation center of a four-circle diffractometer. Each pixel contains a 320- μ m-thick silicon sensor, followed by a charge-sensitive amplifier, a single-level discriminator and a 20-bit counter. An individual pixel is operated in the single-photon counting mode, and the resulting data is free of crosstalk between pixels. Hence, the apparatus provides an angular resolution of 0.007559°, corresponding to one pixel (172 \times 172 μ m²) of the two-dimensional detector. The sample was fixed during exposure, typically for a duration of 100 s. The sample was cooled to 7 K by a refrigerator mounted on the diffractometer. Temperature stability was

*E-mail: kina@eng.hokudai.ac.jp

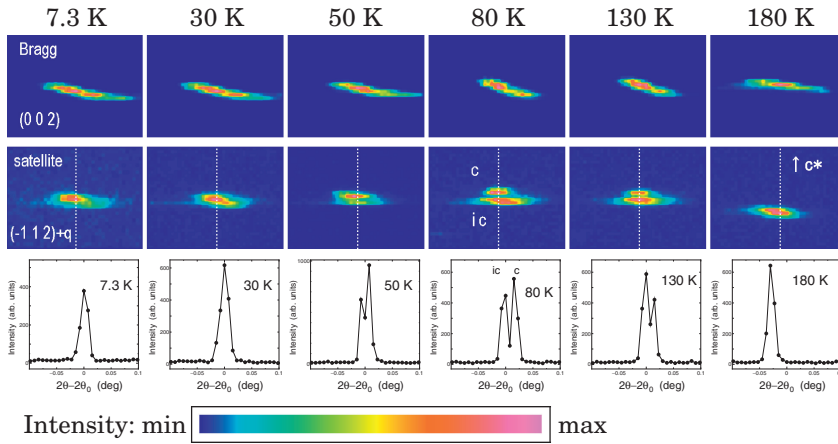


Fig. 1. Bragg (top) and satellite (middle) profiles obtained at 180, 130, 80, 50, 30, and 7.3 K for a *o*-TaS₃ crystal. Vertical axes in the intensity maps denote the c^* -direction. The cross section of each satellite profile along the c^* -direction (white dotted line) is shown in the bottom panels. Here, $2\theta_0$ is the center of the detector. The shape of the Bragg peak shows no significant change; that of the satellite peak evolves with decreasing temperature. The two peaks at 80 K are attributed to the commensurate and incommensurate CDWs, denoted *c* and *ic*, respectively.

maintained within ± 0.01 K in the temperature range of the measurement. The sample was thermally connected with a heat anchor, and the temperature increase by Joule heating was less than 1 K even at the largest current (30 μ A at 80 K). Before each measurement, several reciprocal points were scanned to assign the peaks in order to prevent from confusing it with any spurious signals.

Figure 1 shows the temperature evolution of the Bragg (002) and satellite $(-1, 1, 2) + \mathbf{q}$ peaks obtained at 180, 130, 80, 50, 30, and 7.3 K. The position of the satellite peak was determined to be $\mathbf{q} = (0.5, 0.125, 0.25)$, which agrees with the results of previous studies^{8,11} within experimental errors. We also confirmed that the intensity of the satellite peak rapidly decreases at temperatures higher than the Peierls transition temperature.

The predominant feature in the satellite profiles is the change in the number of peaks (Fig. 1). When the system undergoes Peierls transition at 218 K, a satellite peak begins to develop in intensity and correlation. The initial position of the peak lies around $q_c = (0.255 \pm 0.002)c^*$. When we reduced temperature, a second peak emerged close to the first. This second peak appeared at 130 to 50 K, while at temperatures below 50 K the number of peaks returned to unity. The difference between the two q 's is only $1.3 \times 10^{-3}c^*$, or two pixels at the detector; however, this is still larger than the spatial resolution of the experiment (i.e., ~ 1 pixel). In addition, since no anomalies were found in the Bragg peaks in the whole temperature range, we can rule out the possibility of the presence of any artifacts.

The positions of the two q 's at 80 K were assigned to be $q_c = (0.252 \pm 0.002)c^*$ and $q'_c = (0.250 \pm 0.002)c^*$, where q and q' denote the satellites for higher and lower temperatures, respectively. Hence, the CDWs at higher and lower temperatures are assigned as incommensurate and commensurate, respectively. The result should be compared with known behavior of *o*-TaS₃. In a previous X-ray study,⁸ it was shown that the wave vector at around T_P is incommensurate, $q_c \sim (0.255 \pm 0.003)c^*$, and by reducing temperature it becomes nearly commensurate below 100 K, where $q_c \sim (0.250 \pm 0.004)c^*$. The error bars were mainly the result of the resolution of the experimental setup used at that time. For example, the full width at half maximum of the diffraction peak was as large as $0.01c^*$ in the experiment described in ref. 11; however, our synchrotron study has an advantage in terms of the sharpness of the beam, which leads

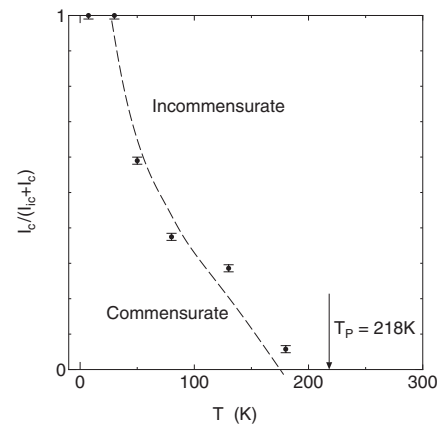


Fig. 2. Phase diagram of *o*-TaS₃ deduced from this study. Solid circles represent the intensity of a commensurate CDW, I_c , normalized by the total intensity of both the commensurate and incommensurate satellites, $I_c + I_{ic}$. The commensurate CDW begins to develop at around 130 K. The two q 's of the CDW coexist until 30 K, at which the entire condensate undergoes an incommensurate–commensurate transition.

to a resolution better than $1 \times 10^{-3}c^*$. In this context, our data can be understood as a natural extension of the previous results.

Details of the incommensurate–commensurate transition were investigated through the intensity evolution of the two CDWs. The use of the Pilatus detector¹⁰ facilitates the determination of the intensity of the peaks. Since the detector contains a two-dimensional array of photon counters, the signal of each pixel is directly proportional to the intensity of incident X-rays. Hence, the intensity of each peak can be obtained simply by numerical integration from the two-dimensional profile. Statistic error of the intensity is estimated as \sqrt{N} , where N is the number of detected photons. In typical experiments, $N \sim 10^4$, resulting in a relative error of $\sqrt{N}/N \sim 10^{-2}$.

Figure 2 shows the relative intensity of the commensurate CDW ($q'_c = 0.250c^*$) normalized by the total satellite intensity, $I_c/(I_{ic} + I_c)$. The broken line in the figure is a guide for the eyes. It is shown that at 50–130 K, where two CDWs coexist, the intensity of the commensurate CDW increases at lower temperatures. The main difference revealed in this study is that the incommensurate CDW is not locked to be commensurate, although its wave vector approaches that of the commensurate CDW. The commen-

surate CDW begins to appear separately at around 130 K and develops at lower temperatures.

Let us compare this observation with those of previous transport studies of *o*-TaS₃. Takoshima *et al.* reported an anomalous increase in longitudinal conductivity below 100 K and attributed it to soliton transport.¹² Although the observation was made before the temperature dependence of the wave vector was measured,⁸ the onset temperature of the anomaly roughly coincides with the appearance of the commensurate CDW. Our data also support the results of the previous study,⁸ and in addition, the observed extension of discommensuration is consistent with the soliton transport concept. Moreover, Zaitsev–Zotov found that there are two kinds of nonlinear conduction in thin samples of *o*-TaS₃. One is a sliding motion, which is observed at high temperatures, and the other results from the quantum creep of the wavefront observed at low temperatures.¹³ This is also easily understood if we accept that two kinds of CDWs can coexist in *o*-TaS₃, as shown in Fig. 2.

Since the longitudinal wave vector q_c is very close to being commensurate, it is important to discuss the possibility of discommensuration. If the wavenumber $2k_F$ is very close to the commensurate length Ma , where M is an integer, and a is the lattice constant, discommensuration will occur per length l_s .⁷ This length is naively related to the difference between the CDW wave vector and the commensurate length, as expressed by

$$\delta q = 2\pi/Ml_s. \quad (1)$$

In our case, $M = 4$ and $\delta q = q_c - q'_c = 0.002c^*$. This gives the mean separation between discommensurations $l_s = 418$ Å. We will discuss this issue in detail later.

We investigated the current dependence of the satellite profile to reveal the nature of each peak. Figure 3 shows the Bragg and satellite profiles at currents of 0 and 30 μA obtained at 80 K. Again, no significant change was observed in the Bragg peak, whereas the satellite peak profile depends on current. At this temperature, the threshold current of the CDW was 6 μA (or a threshold electric field of 0.1 V/cm). Hence, the observed change in the satellite profile should reflect the collective motion of the CDW.

A comparison of the 0 and 30 μA profiles of the satellite peak reveals several remarkable phenomena. The intensities of both peaks of the 0 μA profile appear similar, while those of the 30 μA peak exhibit significant differences, in that the intensity of the top peak (commensurate) decreased while that of the bottom peak (incommensurate) increased. The evolution of the two peaks is shown in detail in Fig. 4. An increase in flowing current increases the intensity of the incommensurate peak, while that of the commensurate peak decreases [Fig. 4(b)]. At 6 μA , a hump (a dip) was observed

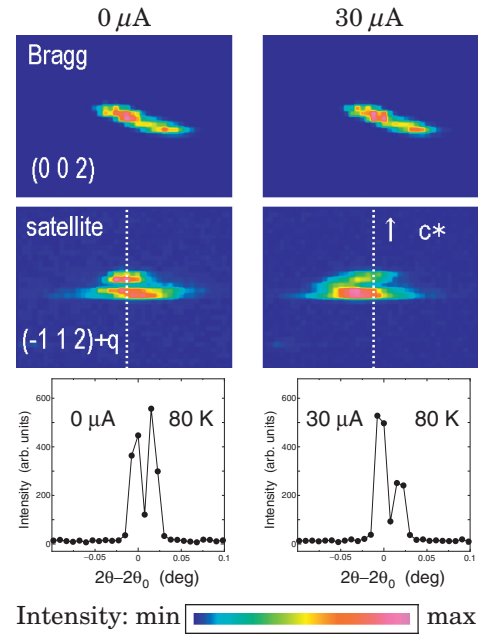


Fig. 3. Current dependence of the Bragg and satellite profiles obtained at 80 K. The legends are the same as those in Fig. 1.

for the incommensurate (commensurate) CDW, and at a larger current, the discrepancy decreases slightly.

In addition to the intensity evolution, the observed peak width also exhibits interesting behavior. Figure 4(c) shows the transverse (across the current flow) peak width for both peaks. The width of the incommensurate satellite decreased from 0.07 to 0.05° at 0 and 6 μA , respectively. Since the transverse peak width is inversely proportional to the length of the correlation, the observed data imply that the transverse correlation is broadened by a factor of 1.4. In contrast, the transverse peak width of the commensurate CDW does not change significantly.

We illustrate the change in transverse correlation length schematically in Fig. 5. As discussed above, there are discommensurations, namely defects in the incommensurate CDW. Since the two CDWs have different wave vectors, there must be a misalignment of wavefronts at the border between these CDWs. In our case, since q in the incommensurate CDW is larger than that in the commensurate CDW, it is possible for dislocations to be located between them. In Fig. 5, the solid lines represent the wavefront, and the hatched circles represent edge dislocations in the phase. There are additional wavefronts between two discommensurations.

The observed change in the peak profile can be understood if the length of the discommensurations is increased,

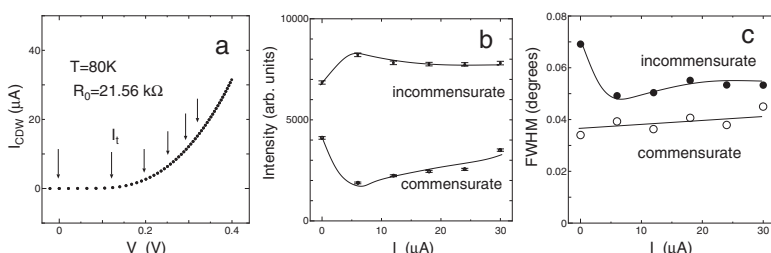


Fig. 4. (a) Charge density wave current as a function of applied voltage at 80 K. The arrows indicate the points at which diffraction was obtained. (b) The intensities of satellite peaks of incommensurate (solid circles) and commensurate (open circles) CDWs. (c) Transverse peak widths of incommensurate (solid circles) and commensurate (open circles) CDWs. The solid lines in (b) and (c) are guides for the eyes.

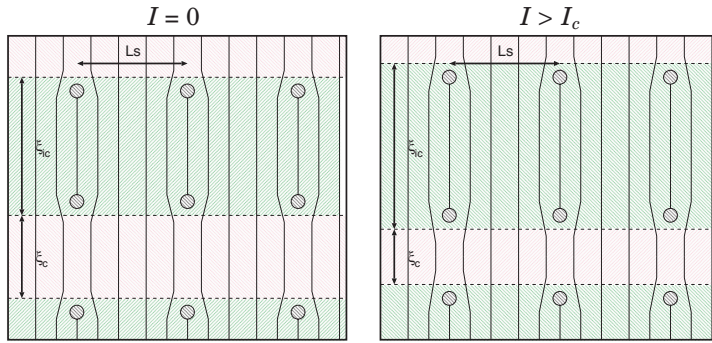


Fig. 5. Schematic illustrations of the evolution of two coinciding CDWs. The solid lines represent the CDW wavefront. The hatched circles indicate edge defects in the CDW phase. There are additional wavefronts between the two defects, or discommensurations at a distance l_s . The widths of the commensurate and incommensurate CDWs are denoted ξ_c and ξ_{ic} , respectively. By inducing a current flow, the lengths of the discommensurations are stretched, resulting in the expansion of the incommensurate CDW.

resulting in the expansion of the incommensurate CDW. At present, there is no microscopic mechanism that agrees quantitatively with the observed phenomena. However, it is worth noting that the edge dislocations in a CDW move easily in the transverse direction.¹⁴ For complete understanding, we must determine the force exerted on the dislocations when the CDW is in motion, thus increasing the portion of the incommensurate CDW. The key to what might lie in the concept of the “type-II CDW” introduced by Hayashi and Yoshioka.² They suggested that dislocations can penetrate a CDW and screen the applied transverse field. This is analogous to the role of vortices in a superconductor. Although previous analyses of the type-II CDW have mainly focused on incommensurate CDW systems, the approach will provide a suitable explanation of the the observed temperature and current dependence of CDW evolution.

We undertook a synchrotron X-ray study of *o*-TaS₃ crystal down to 7 K. Our observation settles an old but open question about the CDW phase in *o*-TaS₃. We found that two kinds of CDWs coexist in the 50–130 K temperature range, and attributed them to commensurate and incommensurate wave vectors. From the electric current dependence of the intensities of both CDWs, we determined the configuration of edge dislocations of the CDW. This picture is more sophisticated than the first prediction of discommensuration.⁷ We have demonstrated that the ratio of commensurate intensity to incommensurate intensity is a function of applied field. As a result, this method will provide a powerful tool for the investigation of commensurate–incommensurate competitions. This work will also have an impact on related topics. For instance, the “1/8 problem” of high- T_c superconductors is now understood as the commensurate lock-in of dynamical stripe order.¹⁵ Future studies of *o*-TaS₃, particularly at low temperatures and with reduced dimensions, will reveal a detailed picture of the nature of dislocation dynamics.

Acknowledgments

This work is partly supported by a Grant-in-Aid for the 21st Century COE program, “Topological Science and Technology”. The authors are grateful for the intensive use of the SPring-8 beamline BL02B1 through project number 2007A0010.

- 1) A. A. Abrikosov: *Zh. Eksp. Teor. Fiz.* **32** (1957) 1442 [Translation: *Sov. Phys. JETP* **5** (1957) 1174].
- 2) M. Hayashi and H. Yoshioka: *Phys. Rev. Lett.* **77** (1996) 3403.
- 3) P. W. Anderson: *Basic Notions of Condensed Matter Physics* (Addison-Wesley, Reading, MA, 1984).
- 4) E. Sweetland, A. C. Finnefrock, W. J. Podulka, M. Sutton, J. D. Brock, D. DiCarlo, and R. E. Thorne: *Phys. Rev. B* **50** (1994) 8157.
- 5) K. L. Ringland, A. C. Finnefrock, Y. Li, J. D. Brock, S. G. Lemay, and R. E. Thorne: *Phys. Rev. B* **61** (2000) 4405.
- 6) R. Danneau, A. Ayari, D. Rideau, H. Requardt, J. E. Lorenzo, L. Ortega, P. Monceau, R. Currat, and G. Grübel: *Phys. Rev. Lett.* **89** (2002) 106404.
- 7) W. L. McMillan: *Phys. Rev. B* **14** (1976) 1496.
- 8) C. Roucau: *J. Phys. (Paris)* **44** (1983) C3-1725.
- 9) The experimental configuration in this study provided a bulk behavior of the CDW. Hence our observation differs qualitatively from those of spatially resolved X-ray studies of CDWs: D. DiCarlo, E. Sweetland, M. Sutton, J. D. Brock, and R. E. Thorne: *Phys. Rev. Lett.* **70** (1993) 845; D. Rideau, P. Monceau, R. Currat, H. Requardt, F. Nad, J. E. Lorenzo, S. Brazovskii, C. Detlefs, and G. Grübel: *Europhys. Lett.* **56** (2001) 289; D. Le Bolloc’h, S. Ravy, J. Dumas, J. Marcus, F. Livet, C. Detlefs, F. Yakhou, and L. Paolasini: *Phys. Rev. Lett.* **95** (2005) 116401.
- 10) H. Toyokawa, M. Suzuki, Ch. Brönnimann, E. F. Eikenberry, B. Henrich, G. Hülsen, and P. Kraft: *AIP Conf. Proc.* **879** (2007) 1141.
- 11) K. Tsutsumi, T. Sambongi, S. Kagoshima, and T. Ishiguro: *J. Phys. Soc. Jpn.* **44** (1978) 1735.
- 12) T. Takoshima, M. Ido, K. Tsutsumi, T. Sambongi, S. Honma, K. Yamaya, and Y. Abe: *Solid State Commun.* **35** (1980) 911.
- 13) S. V. Zaitsev-Zotov: *Phys. Rev. Lett.* **71** (1993) 605.
- 14) N. P. Ong and K. Maki: *Phys. Rev. B* **32** (1985) 6582.
- 15) S. A. Kivelson, I. P. Bindloss, E. Fradkin, V. Oganesyan, J. M. Tranquada, A. Kapitulnik, and C. Howald: *Rev. Mod. Phys.* **75** (2003) 1201.